



Su, Weiguang and Darkwa, Jo and Kokogiannakis, Georgios (2017) Development of microencapsulated phase change material for solar thermal energy storage. *Applied Thermal Engineering*, 112 . pp. 1205-1212. ISSN 1873-5606

**Access from the University of Nottingham repository:**

<http://eprints.nottingham.ac.uk/47443/1/10.1016%40j.applthermaleng.2016.11.009.pdf>

**Copyright and reuse:**

The Nottingham ePrints service makes this work by researchers of the University of Nottingham available open access under the following conditions.

This article is made available under the Creative Commons Attribution Non-commercial No Derivatives licence and may be reused according to the conditions of the licence. For more details see: <http://creativecommons.org/licenses/by-nc-nd/2.5/>

**A note on versions:**

The version presented here may differ from the published version or from the version of record. If you wish to cite this item you are advised to consult the publisher's version. Please see the repository url above for details on accessing the published version and note that access may require a subscription.

For more information, please contact [eprints@nottingham.ac.uk](mailto:eprints@nottingham.ac.uk)

# Accepted Manuscript

Research Paper

Development of microencapsulated phase change material for solar thermal energy storage

Weiguang Su, Jo Darkwa, Georgios Kokogiannakis

PII: S1359-4311(16)32969-6

DOI: <http://dx.doi.org/10.1016/j.applthermaleng.2016.11.009>

Reference: ATE 9414

To appear in: *Applied Thermal Engineering*

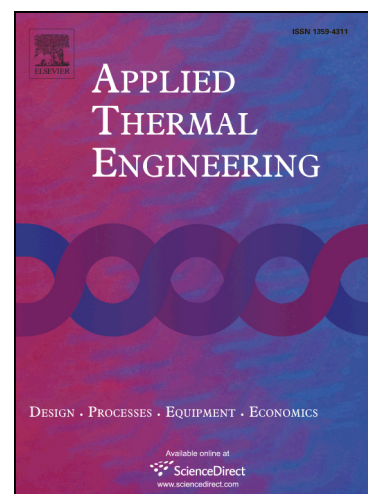
Received Date: 31 August 2016

Revised Date: 23 October 2016

Accepted Date: 1 November 2016

Please cite this article as: W. Su, J. Darkwa, G. Kokogiannakis, Development of microencapsulated phase change material for solar thermal energy storage, *Applied Thermal Engineering* (2016), doi: <http://dx.doi.org/10.1016/j.applthermaleng.2016.11.009>

This is a PDF file of an unedited manuscript that has been accepted for publication. As a service to our customers we are providing this early version of the manuscript. The manuscript will undergo copyediting, typesetting, and review of the resulting proof before it is published in its final form. Please note that during the production process errors may be discovered which could affect the content, and all legal disclaimers that apply to the journal pertain.



# Development of microencapsulated phase change material for solar thermal energy storage

Weiguang Su<sup>1,a</sup>, Jo Darkwa<sup>2</sup>, Georgios Kokogiannakis<sup>3</sup>

1. School of Mechanical & Automotive Engineering, Qilu University of Technology, Jinan, China
2. Faculty of Engineering, University of Nottingham, UK
3. Sustainable Buildings Research Centre, University of Wollongong, Australia

## Nomenclature

$Cp_w$ , $Cp_{PCM}$ , $Cp_s$	the specific heat of water, core material and shell material
$H_{PCM}$	latent heat of PCM
$H$	enthalpy
$k_w$ , $k_{PCM}$ , $k_s$	the conductivity of water, paraffin and shell material
$wt_w$ , $wt_{PCM}$ , $wt_s$	the weight percentage of water, core material and shell material
$wt_{ME}$	the weight percentages of MEPCM in TES unit
$\varphi_w$ , $\varphi_s$ , $\varphi_{PCM}$	the volume percentage of water, shell material and core material
$\Delta T$	the temperature difference
$\emptyset$	the core material content of MEPCM

---

<sup>a</sup> Corresponding author. E-mail address: wgsuper@hotmail.com

## 1 Introduction

Solar thermal energy storage (TES) systems are considered to be among the commonest methods of providing hot water or space heating services in buildings due to their relatively lower cost and ease of operation [1-3]. For instance, a seasonal solar TES water tank was used to improve the energy performance of district heating/cooling and hot water supply systems by Tanaka et al [4]. Furbo et al.[5] developed a smart solar TES tank for a small solar domestic hot water system, which can be heated both by solar collectors and by means of an auxiliary energy supply system. The investigations showed that the yearly thermal performance of the smart solar system was 5–35% higher than traditional system. However, the TES tanks do experience buoyancy dependent stratification which tends to affect their heat transfer processes [6-8]. They also tend to be relatively bulky and occupy more useable space[9]. To this end, Morrison *et al.* [8] have investigated the use of mantle heat exchangers as means of degrading thermal stratification in TES tanks and thereby enhancing the thermal performance of solar water heating systems. Various researchers have also explored the possibility of using phase change materials (PCMs) as heat storage media since they have much higher energy storage capacity and energy storage density than water [2, 10-13]. For instance, Murray and Groulx [10] evaluated a PCM based TES system and achieved about 44.3% increase in energy storage density as compared with water based system. Similar investigation carried out by Delgado et al.[13] with PCM emulsion, also achieved an increase of 34% in energy storage capacity as against water based TES system.

However, PCMs generally possess low thermal conductivity and hence poor thermal response factor. For example the study by López-Navarro *et al.* [14] showed a declining thermal response factor in a PCM storage tank after a few number of thermal cycling and was attributed to low thermal conductivity of the PCM. Other general weakness in PCMs is instability in their melting temperatures during long term storage operation. This phenomena was evident in a study by Behzadi [15] when the melting temperature of the PCM shifted from 21 to 28°C after 120 repeated thermal cycles. Apart from thermal instability issue, Chen *et al.* [16] also observed a high level of thermal stress in a PCM storage tank as a result of considerable change in density during phase transition period.

In order to overcome some of these problems the study was primarily focused on the development of a novel high temperature microencapsulated phase change material (MEPCM) for application in a compacted water saturated fixed bed system [12] as shown in Fig. 1. This storage unit has the potential of achieving much higher effective thermal conductivity, enhanced thermal stability and higher energy storage density with a relatively smaller physical storage size than conventional water storage tanks.

## 2 Development of MEPCM

### 2.1 Material selection

Paraffin wax with a melting temperature of 48°C was chosen as the base material for the development of the MEPCM because of its relatively high latent heat capacity and phase change temperature. Melamine-formaldehyde (MF) resins have been widely used as shell materials for encapsulation processes due to their ability to be crosslinked at different melamine/formaldehyde molecular ratios such as: 1:1.25-2 [17], 1:2.66 [18] and 1:2.5 [19]). Therefore melamine with 99% purity level and 37 wt% formaldehyde solution was used as shell monomers. Two types of emulsifiers i.e. Sodium dodecyl sulfate (SDS; Sinopharm Chemical Reagent Co.,Ltd, China; purity 90%) and binary emulsifier Brij 30 (Aladdin, Japan) & Brij 58 (Sigma, USA) were used to evaluate the effect of emulsifiers on the developed MEPCM. Citric acid (Sinopharm Chemical Reagent Co.,Ltd, China) and sodium hydroxide (Sinopharm Chemical Reagent Co.,Ltd, China) solution were used to control the pH values during the experimental process. Ammonium chloride (purity 99.5%) also supplied by Sinopharm Chemical Reagent Co.,Ltd. was used as a nucleation agent whereas deionized water was applied for dilution processes. Table 1 shows a summary and composition of basic materials that were used for the development of the MEPCM samples (MF-1, MF-2, MF-3, MF-4 and MF-5).

## 2.2 Fabrication of MEPCM

The fabrication of the MEPCM samples was based on in-situ polymerization method as well as processes covering synthesis of prepolymer solution, preparation of oil-in-water (O/W) emulsion and formation of shells. The value of hydrophilic-lipophilic balance (HLB) [20] of emulsifier is one of the most important factors for preparing a stable oil-in-water (O/W) emulsion. Meanwhile, the average HLB value for the nonionic binary emulsifier can be calculated according to the weight percentages and HLB values of the initial components [21]. Therefore Brij 30 and Brij 58 were mixed together at an appropriate HLB value of 12 to prepare for the O/W emulsion. As shown in Fig. 2, melamine (4.04g) and 37% formaldehyde solution (6.5g) were initially mixed with 10ml deionized water at a stirring speed of 200 rpm. It was then heated up to 70°C and maintained at that reaction temperature until the suspension became transparent. The prepolymer solution was prepared at a pH value of 8.5–9 with 0.2wt% sodium hydroxide solution. The next stage of the fabrication process involved mixing together the molten paraffin with deionized water and the emulsifiers. The solution was then stirred at a speed of 7000rpm for 10min with a dispersion machine (IKA T18, Germany, see Fig.3) to obtain a stable O/W emulsion. In order to fabricate the MEPCM, the capsules need to crosslink with MF polymer at a lower pH value ranging from 3-5 as shown in the fabrication flow chart. For this reason the pH value of the mixture was modified to 3–4 with 5wt% citric acid solution to initiate the crosslinking process. Meanwhile the prepolymer solution was added to the O/W emulsion at a stirring speed of 300

rpm with a magnetic stirrer (type IKA HS-7, Germany, see Fig.3) for 4 hours at a temperature of 70°C. The end product was finally filtered, washed with water and then dried in an oven at a temperature of 60°C for 20 hours.

### **3 Results and analysis**

#### **3.1 Evaluation of fabricated MEPCM samples**

##### **3.1.1 Scanning electron microscopy (SEM) analysis**

A scanning electron microscope (SEM) by Sigma VP, Carl Zeiss Co. Ltd., was used to examine the morphologies of the fabricated MEPCM samples. Since the shell material is a non-conductive material, the samples were initially coated with 5 nm thick gold layer in order to increase their electrical conductivity before the microscopy analysis was carried out. This procedure was in accordance with a similar study carried out by Suzuki [22].

As shown in Fig. 4, the particles sizes of the samples were similar in sizes measuring about 2 $\mu$ m but there were significant differences in their morphologies which were attributed to different HLB values for the emulsifiers used for the encapsulation process. For instance the HLB value for the anionic SDS emulsifier used for samples MF-1, MF-2 and MF-3 (Fig. 4a to Fig. 4c) was as high as 40 which resulted in the agglomeration of the particles. On the other hand the MF-4 and MF-5 samples (Fig. 4d and Fig. 4e) achieved much better morphologies with a lower HLB value of 12 for



the binary emulsifiers (Brij 30 and Brij 58). In general emulsifiers are used for reducing interfacial tension in O/W emulsions and to prevent coalescence by capsules adsorption onto the oil/water interface in order to promote the formation of regular shapes of capsules during microencapsulation process. It is obvious from the outcomes that the binary emulsifiers were more effective than the SDS emulsifier due to the synergy of the two emulsifiers [23] hence.

### **3.1.2 Energy storage capacity, melting temperature and encapsulation efficiency**

A differential scanning calorimetric (DSC6220, SII Nanotechnology) equipment was used in determining the enthalpies of fusion and melting temperature of the MEPCM samples in accordance with ISO 11357 Standards under the dynamic testing method. The samples were tested at atmospheric pressure and at a heating rate of 2 °C /min from 5°C to 65°C.

As shown in Fig. 5 and in relation to the pure paraffin, sample MF-3 achieved the highest melting enthalpy of 126 kJ/kg as against 57 kJ/kg, 84.3kJ/kg, 95.8 kJ/kg and 104 kJ/kg for MF-1, MF-2, MF-4 and MF-5 respectively. With regard to their melting temperatures, there was no strong evidence to suggest that the organic emulsifiers had any major effect on the samples since there was only a slight reduction of between 0.08°C to 0.95°C as summarized in Tab. 2. The DSC results were also used to determine the encapsulation efficiency which is defined as the ratio of the actual core content of the microcapsules to the theoretical core content [24]. The percentages of

core material contents for the samples were therefore obtained as 29% for MF-1, 43% for MF-2, 65% for MF-3 49% for MF-4 and 54% for MF-5. Now based on the initial core/shell weight ratios in Tab. 1, the corresponding encapsulation efficiencies were obtained as 44.23%, 65.18%, 97.42%, 74.07% and 80.41%.

Beside the morphology the type of emulsifiers also demonstrated some effects on the core material content and encapsulation efficiency for the fabricated MEPCM samples. For instance, the core material content for sample MF-4 (49%) was much higher than sample MF-1 (29%) due to the effect of the binary emulsifier. However, comparison of MF-5 and MF-3 shows that the core material content was reduced about 11% by the binary emulsifier, which was attributed to the fact that some of the capsules in MF-5 were not fully encapsulated.

The results as summarised in Tab. 2 show that the nucleating agent (ammonium chloride) did also influence the core material content and the encapsulation efficiencies of the MEPCM samples. For instance the core material content and the encapsulation efficiency for MF-3 did increase by more than 35% and 53% respectively with 0.25g of ammonium chloride as a nucleation agent. Meanwhile, the core material content and the encapsulation efficiency of MF-5 also increased by 5%-6% thus showing the positive effect of nucleating agent when the binary emulsifiers were used to prepare the MEPCM samples. This is based on the fact that ammonium chloride as nucleating agent can effectively reduce the pH value [25] during the polymerization reaction.

### 3.1.3 Thermal stability

Thermogravimetric (TG) technique can be used to analyse the thermal stability of a sample material by measuring the amount of weight change of the material as a function of increasing temperature in a controlled atmosphere of nitrogen, helium, air, or in vacuum, which exhibits loss or gain of mass due to thermal decomposition, evaporation, oxidation or dehydration of the sample [26]. The thermal stabilities of the MEPCM samples were therefore examined under nitrogen gas protection covering a heating range of 50°C to 500°C and at a heating rate of 10°C/min. As presented in Fig. 6, the maximum weight loss temperatures for the samples were as high as 283.7°C, 280.1°C, 279.7°C, 283°C and 272.2°C for MF-1, MF-2, MF-3, MF-4 and MF-5 respectively as compared with 238°C for the pure paraffin. It should also be noted that in general higher core material content does affect the thermal stability of capsules thus confirming why MF-5 achieved the lowest weight loss temperature. Even though the shell material of the samples has a lower melting point temperature of 180°C than the corresponding weight loss temperatures, it is far more higher than the temperature requirement for hot water (29–60°C) [27] or space heating (30-65°C) [28] services in buildings. In addition the shell material can protect the core material from the influences of the outside environment and to maintain temperature stability for long term TES application. Above all the MF shell can accommodate changes in volume during phase change process of the core material thereby decreasing the thermal stress in TES tanks. Therefore, the long term operational thermal stability of the latent

heat storage media for the proposed TES unit can be improved by using the developed MEPCM.

### 3.2 Theoretical evaluation of proposed TES unit

As described in Fig. 1, the TES unit is similar to the concept adopted for enhancing energy storage density and effective thermal conductivity in a study conducted by Darkwa *et al.* [29]. Therefore by considering individual elements and their weight proportions the various percentages of energy storage capacity may be calculated using Eq. 1 below as:

$$H = wt_w \cdot Cp_w \cdot \rho_w \cdot \Delta T + wt_{PCM} \cdot (Cp_{PCM} \cdot \Delta T + H_{PCM}) \cdot \rho_{PCM} + wt_s \cdot Cp_s \cdot \rho_s \cdot \Delta T \quad (1)$$

$$wt_w + wt_{PCM} + wt_s = 1 \quad (2)$$

$$wt_{PCM} = wt_{ME} \cdot \phi \quad (3)$$

$$wt_s = wt_{ME} \cdot (1 - \phi) \quad (4)$$

So that Eq.1 becomes:

$$H = Cp_w \rho_w \Delta T + wt_{ME} [\phi (Cp_{PCM} \cdot \Delta T + H_{PCM}) \rho_{PCM} + (1 - \phi) Cp_s \rho_s \Delta T - Cp_w \rho_w \Delta T] \quad (5)$$

Where

$wt_w$ ,  $wt_{PCM}$  and  $wt_s$  are the weight percentages of water, core material and shell material respectively, %.

$Cp_w$ ,  $Cp_{PCM}$  and  $Cp_s$  are the corresponding specific heat capacities, J/kg·°C.

$\rho_w$ ,  $\rho_{PCM}$ , and  $\rho_s$  are the corresponding densities, kg/m<sup>3</sup>.

$H_{PCM}$  is the latent heat of PCM, kJ/kg.

$\Delta T$  is the temperature difference, °C.

$wt_{ME}$  is the weight percentages of MEPCM in TES unit, %.

$\emptyset$  is the core material content of MEPCM, %.

The effective thermal conductivity can also be calculated by considering the conductivity and the volume fraction of each component as established by Thiele *et al.* [30] and reported by Felske [31] in Eq. 6 as:

$$k_e = \frac{2k_w(1-\varphi_s-\varphi_{PCM})\left(3+2\frac{\varphi_s}{\varphi_{PCM}}+\frac{\varphi_s k_{PCM}}{\varphi_{PCM} k_s}\right) + (1+2\varphi_{PCM}+2\varphi_s)\left[\left(3+\frac{\varphi_s}{\varphi_{PCM}}\right)k_{PCM}+2\frac{\varphi_s k_s}{\varphi_{PCM}}\right]}{(2+\varphi_s+\varphi_{PCM})\left(3+2\frac{\varphi_s}{\varphi_{PCM}}+\frac{\varphi_s k_{PCM}}{\varphi_{PCM} k_s}\right) + (1-\varphi_s-\varphi_{PCM})\left[\left(3+\frac{\varphi_s}{\varphi_{PCM}}\right)\frac{k_{PCM}}{k_w}+2\frac{\varphi_s k_s}{\varphi_{PCM} k_w}\right]} \quad (6)$$

$$\varphi_w + \varphi_{PCM} + \varphi_s = 1 \quad (7)$$

$$\varphi_{PCM} = \frac{\frac{wt_{PCM}}{\rho_{PCM}}}{\frac{wt_{PCM}}{\rho_{PCM}} + \frac{wt_s}{\rho_s} + \frac{wt_w}{\rho_w}} \quad (8)$$

According to Eq.2-4, Eq.7 becomes:

$$\varphi_{PCM} = \frac{\frac{wt_{ME} \cdot \emptyset}{\rho_{PCM}}}{\frac{wt_{ME} \cdot \emptyset}{\rho_{PCM}} + \frac{wt_{ME} \cdot (1-\emptyset)}{\rho_s} + \frac{1-wt_{ME}}{\rho_w}} \quad (9)$$

By the same method,

$$\varphi_s = \frac{\frac{wt_{ME} \cdot (1-\emptyset)}{\rho_s}}{\frac{wt_{ME} \cdot \emptyset}{\rho_{PCM}} + \frac{wt_{ME} \cdot (1-\emptyset)}{\rho_s} + \frac{1-wt_{ME}}{\rho_w}} \quad (10)$$

Where

$k_m$ ,  $k_{PCM}$  and  $k_s$  are the conductivities of water, paraffin and shell material, W/m·K.

$\varphi_w$ ,  $\varphi_s$  and  $\varphi_{PCM}$  are the volume percentages of water, shell material and core material, %.

Now using sample MF-3 and the data in Tab. 3, the energy storage density and the effective thermal conductivity of the TES unit over a range of 40 to 60 °C with different weight percentage of MPEPCM can be calculated and represented graphically in Fig. 7.

Analysis of the results show that energy storage density increases with weight percentage of the MEPCM whilst effective thermal conductivity reduces. For instance if 50 wt% MEPCM is to be used in the proposed TES unit, its energy storage density would increase from 84000 kJ/m<sup>3</sup> to 128735 kJ/m<sup>3</sup>. It would also reduce the volume of the TES unit by about 34.7% in comparison with a water storage tank of the same energy storage capacity. Even though the effective thermal

conductivity of ( $k_{e1}$ ) would reduce to 0.41 W/m·K, it is still about 2 times that of pure paraffin. In comparison with other studies, the effective conductivity of the developed MEPCM is much higher than other thermal energy storage materials, such as lauric acid (0.148~0.150 W/m·K) [10], PCM emulsion (0.27 W/m·K) [13], RT8 (0.20 W/m·K) [14] and Rubitherm 21 (0.20 W/m·K) [15]. Previous investigations also showed that thermal response time of TES units were poor due to low thermal conductivity of the phase change materials. For instance the experimental results by Murray and Groulx [10] showed that the time requirements for thermal energy charging and discharging in a TES system were as long as 30 hours and 32 hours respectively. The thermal response of the proposed TES unit is therefore expected to be much higher during thermal energy charging/discharging cycling. There is however the need for the TES unit to be optimized based on design and operational requirements.

## 4 Conclusions

The study was focused on the development of a high melting temperature MEPCM for solar hot water storage system. Five MEPCM samples (MF-1, MF-2, MF-3, MF-4 and MF-5) have therefore been successfully fabricated through in-situ polymerization method. Analysis of the results showed that MF-3 achieved the highest enthalpy of 126 kJ/kg but there was no huge difference in their melting temperatures which was ranged between 0.08°C to 0.95°C. In general the overall

thermal stability of the samples was relatively high with MF-3 reaching 279.7°C. The encapsulation efficiency was however influenced by the nucleation agent whilst the morphology was also affected by the type of emulsifier since samples MF-4 and MF-5 achieved much better morphology with the binary emulsifier than samples MF-1, MF-2 and MF-3 which were fabricated with SDS emulsifier. In order to assess their thermal effectiveness, MF-3 was theoretically evaluated in an integrated compacted fixed bed unit and found to be capable of contributing to a system with higher energy storage density and relatively smaller physical storage size than water based system. Even though the overall effective thermal conductivity of the unit was slightly less than water, it was found to be about twice as high as most current PCM storage units. The proposed TES unit is therefore expected to be thermally more responsive during thermal energy charging/discharging process. Experimental evaluation is therefore being encouraged towards achieving a workable prototype.

## Reference

- [1] J.F. Belmonte, P. Eguía, A.E. Molina, J.A. Almendros-Ibáñez, R. Salgado, A simplified method for modeling the thermal performance of storage tanks containing PCMs, *Applied Thermal Engineering*, 95 (2016) 394-410.
- [2] S. Seddegh, X. Wang, A.D. Henderson, Z. Xing, Solar domestic hot water systems using latent heat energy storage medium: A review, *Renewable and Sustainable Energy Reviews*, 49 (2015) 517-533.
- [3] M. Thirugnanasambandam, S. Iniyar, R. Goic, A review of solar thermal technologies, *Renewable and Sustainable Energy Reviews*, 14 (2010) 312-322.



- [4] H. Tanaka, T. Tomita, M. Okumiya, Feasibility study of a district energy system with seasonal water thermal storage, *Solar Energy*, 69 (2000) 535-547.
- [5] S. Furbo, E. Andersen, S. Knudsen, N.K. Vejen, L.J. Shah, Smart solar tanks for small solar domestic hot water systems, *Solar Energy*, 78 (2005) 269-279.
- [6] H.Ö. Paksoy, Thermal energy storage for sustainable energy consumption fundamentals, case studies and design, Springer, Dordrecht ;, 2007.
- [7] M. Raisul Islam, K. Sumathy, S. Ullah Khan, Solar water heating systems and their market trends, *Renewable and Sustainable Energy Reviews*, 17 (2013) 1-25.
- [8] G.L. Morrison, A. Nasr, M. Behnia, G. Rosengarten, Analysis of horizontal mantle heat exchangers in solar water heating systems, *Solar Energy*, 64 (1998) 19-31.
- [9] J. Xu, R.Z. Wang, Y. Li, A review of available technologies for seasonal thermal energy storage, *Solar Energy*, 103 (2014) 610-638.
- [10] R.E. Murray, D. Groulx, Experimental study of the phase change and energy characteristics inside a cylindrical latent heat energy storage system: Part 1 consecutive charging and discharging, *Renewable Energy*, 62 (2014) 571-581.
- [11] D.N. Nkwetta, F. Haghghat, Thermal energy storage with phase change material—A state-of-the art review, *Sustainable Cities and Society*, 10 (2014) 87-100.
- [12] M.K.A. Sharif, A.A. Al-Abidi, S. Mat, K. Sopian, M.H. Ruslan, M.Y. Sulaiman, M.A.M. Rosli, Review of the application of phase change material for heating and domestic hot water systems, *Renewable and Sustainable Energy Reviews*, 42 (2015) 557-568.
- [13] M. Delgado, A. Lázaro, J. Mazo, C. Peñalosa, P. Dolado, B. Zalba, Experimental analysis of a low cost phase change material emulsion for its use as thermal storage system, *Energy Conversion and Management*, 106 (2015) 201-212.
- [14] A. López-Navarro, J. Biosca-Taronger, J.M. Corberán, C. Peñalosa, A. Lázaro, P. Dolado, J. Payá, Performance characterization of a PCM storage tank, *Applied Energy*, 119 (2014) 151-162.
- [15] S. Behzadi, M.M. Farid, Long term thermal stability of organic PCMs, *Applied Energy*, 122 (2014) 11-16.
- [16] S.-L. Chen, C.-L. Chen, C.-C. Tin, T.-S. Lee, M.-C. Ke, An experimental investigation of cold storage

in an encapsulated thermal storage tank, *Experimental Thermal and Fluid Science*, 23 (2000) 133-144.

[17] F. Cao, B. Yang, Supercooling suppression of microencapsulated phase change materials by optimizing shell composition and structure, *Applied Energy*, 113 (2014) 1512-1518.

[18] J.K. Choi, J.G. Lee, J.H. Kim, H.S. Yang, Preparation of microcapsules containing phase change materials as heat transfer media by in-situ polymerization, *Journal of Industrial and Engineering Chemistry*, 7 (2001) 358-362.

[19] K. Hong, S. Park, Melamine resin microcapsules containing fragrant oil: synthesis and characterization, *Materials Chemistry and Physics*, 58 (1999) 128-131.

[20] T.F. Tadros, *Emulsion Science and Technology*, Wiley, 2009.

[21] W.C. Griffin, Calculation of HLB values of Nonionic Surfactants, *J. Soc. Cosmet. Chem*, 5 (1954) 249-256.

[22] E. Suzuki, High-resolution scanning electron microscopy of immunogold-labelled cells by the use of thin plasma coating of osmium, *Journal of Microscopy*, 208 (2002) 153-157.

[23] M.J. Rosen, Predicting synergism in binary mixtures of surfactants, in: M.J. Schwuger, F.H. Haegel (eds.) *Surfactants and Colloids in the Environment*, Steinkopff, Darmstadt, 1994, pp. 39-47.

[24] H. Zhang, X. Wang, Synthesis and properties of microencapsulated n-octadecane with polyurea shells containing different soft segments for heat energy storage and thermal regulation, *Solar Energy Materials and Solar Cells*, 93 (2009) 1366-1376.

[25] I.S. Chuang, G.E. Maciel, Carbon-13 CP/MAS NMR study of the structural dependence of urea-formaldehyde resins on formaldehyde-to-urea molar ratios at different urea concentrations and pH values, *Macromolecules*, 25 (1992) 3204-3226.

[26] M.E. Brown, *INTRODUCTION TO THERMAL ANALYSIS: Techniques and Applications*, Springer, Netherlands, 2001.

[27] W. Su, J. Darkwa, G. Kokogiannakis, Review of solid-liquid phase change materials and their encapsulation technologies, *Renewable and Sustainable Energy Reviews*, 48 (2015) 373-391.

[28] D. Feldman, M.M. Shapiro, D. Banu, C.J. Fuks, Fatty acids and their mixtures as phase-change materials for thermal energy storage, *Solar Energy Materials*, 18 (1989) 201-216.

[29] J. Darkwa, O. Su, T. Zhou, Development of non-deform micro-encapsulated phase change energy storage tablets, *Applied Energy*, 98 (2012) 441-447.

[30] A.M. Thiele, A. Kumar, G. Sant, L. Pilon, Effective thermal conductivity of three-component composites containing spherical capsules, *International Journal of Heat and Mass Transfer*, 73 (2014) 177-185.

[31] J.D. Felske, Effective thermal conductivity of composite spheres in a continuous medium with contact resistance, *International Journal of Heat and Mass Transfer*, 47 (2004) 3453-3461.

ACCEPTED MANUSCRIPT

Table 1: Materials for MEPCM fabrication

Table 2: Thermal properties of paraffin and MEPCM samples

Table 3: Thermophysical properties of TES components

Figure 1: Compacted MEPCM bed system for solar TES system

Figure 2: MEPCM fabrication procedure [17-19]

Figure 3: Experimental rig for MEPCM preparation

Figure 4: SEM examination of MEPCM samples

Figure 5: DSC analysis of pure paraffin and MEPCM samples

Figure 6: TG analysis of pure paraffin and MEPCM samples

Figure 7: Thermal profile of TES unit

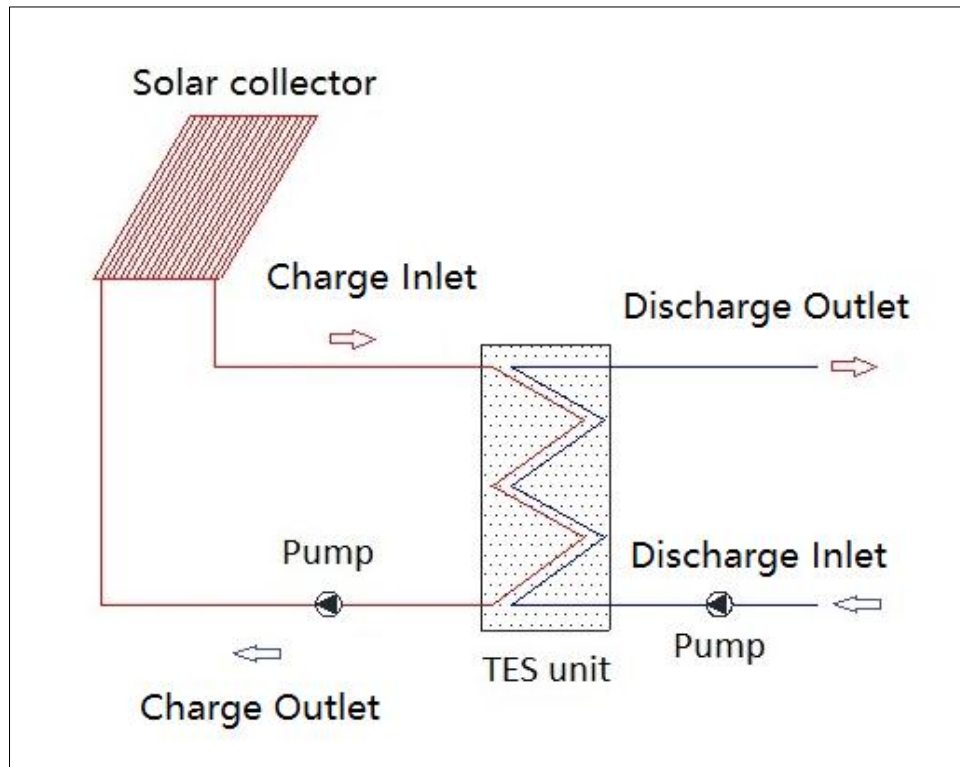


Figure 1: Compacted MEPCM bed system for solar TES system

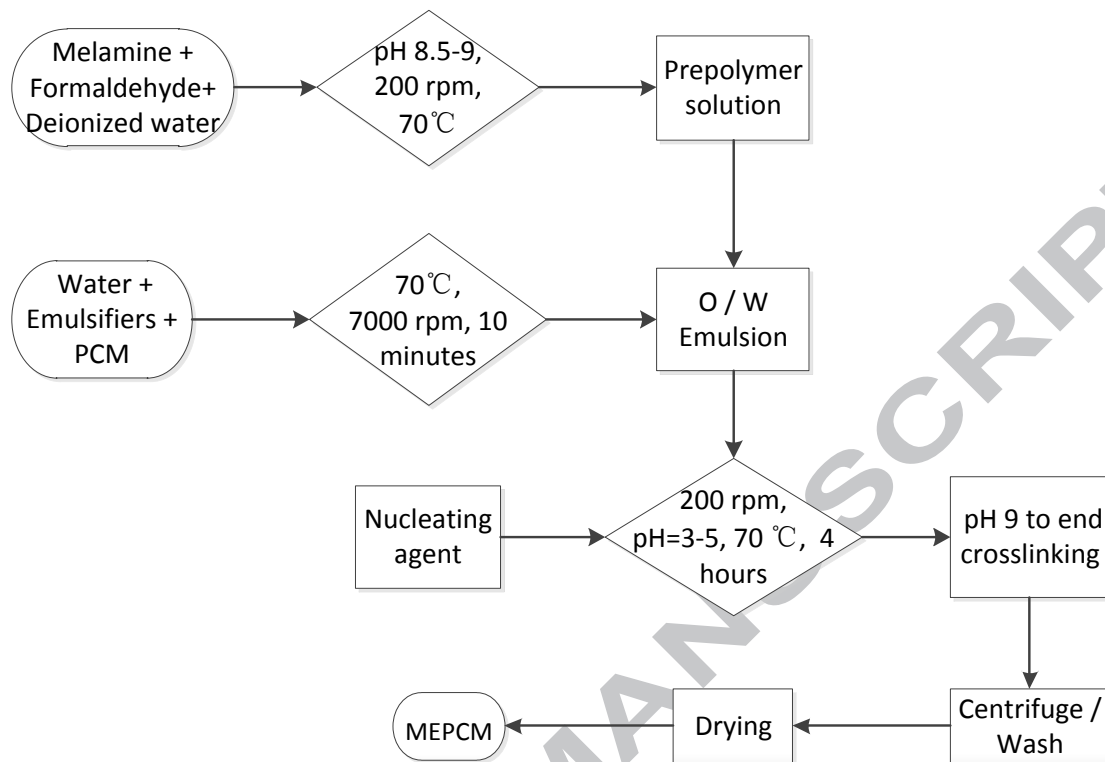


Figure 2: MEPCM fabrication procedure [17-19]

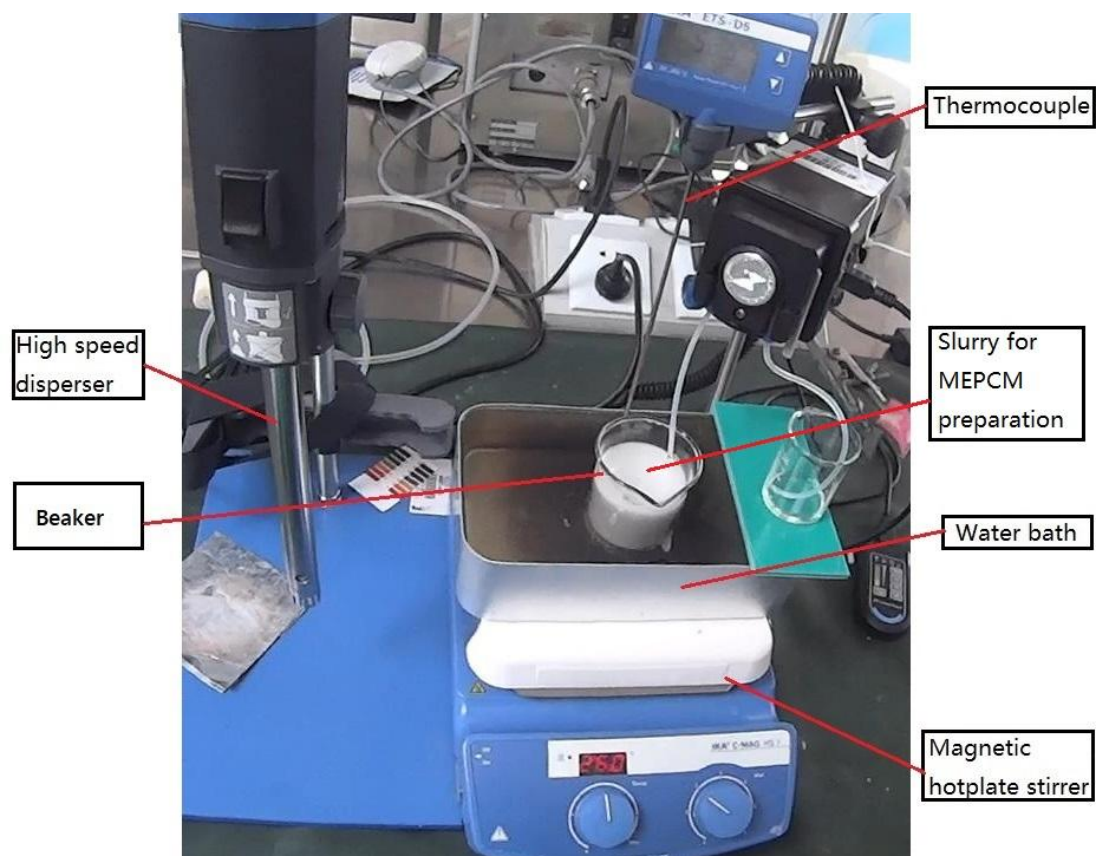
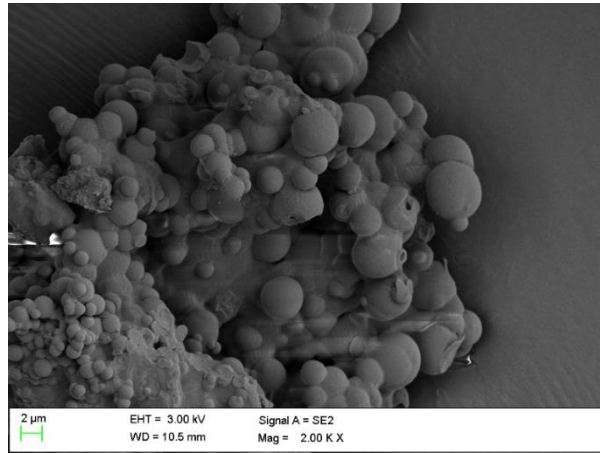
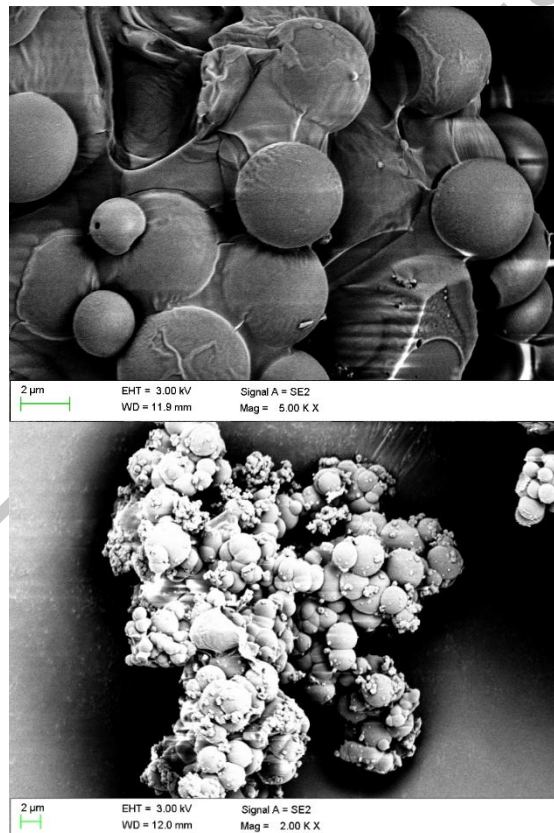


Figure 3: Experimental rig for MEPCM preparation



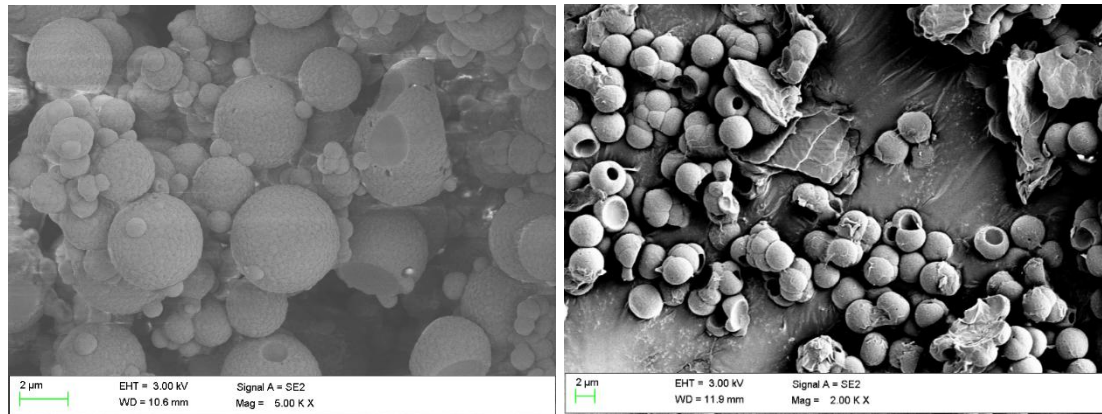
(a) MF-1



(b) MF-2

(c) MF-3





(d) MF-4

(e) MF-5

Figure 4: SEM examination of MEPCM samples

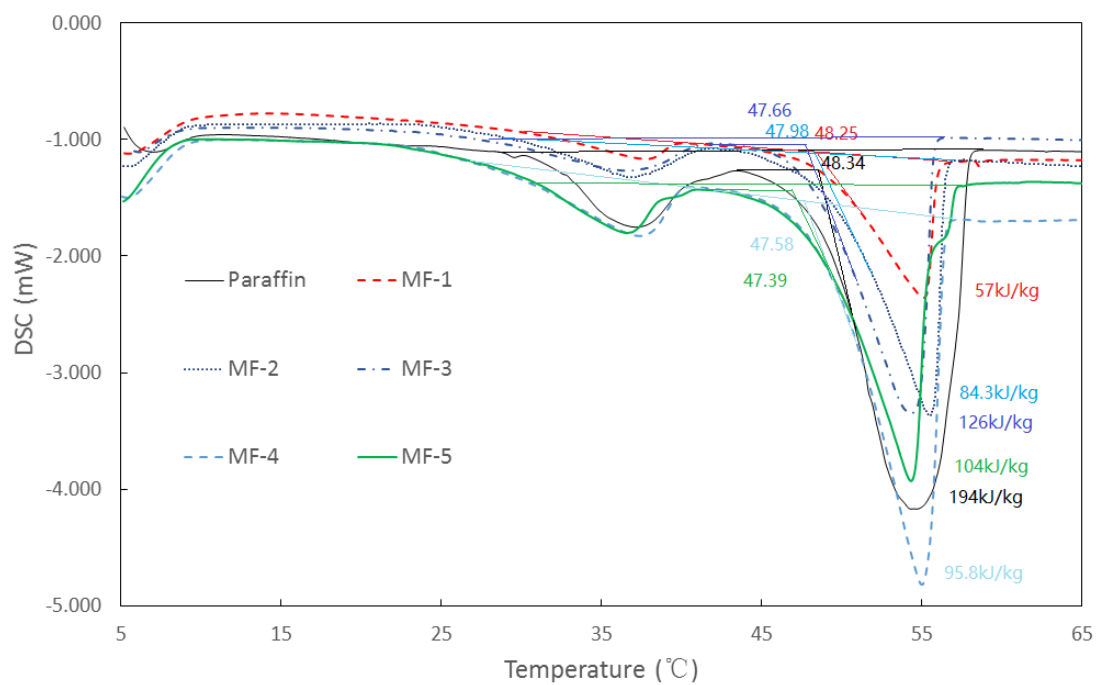


Figure 5: DSC analysis of pure paraffin and MEPCM samples

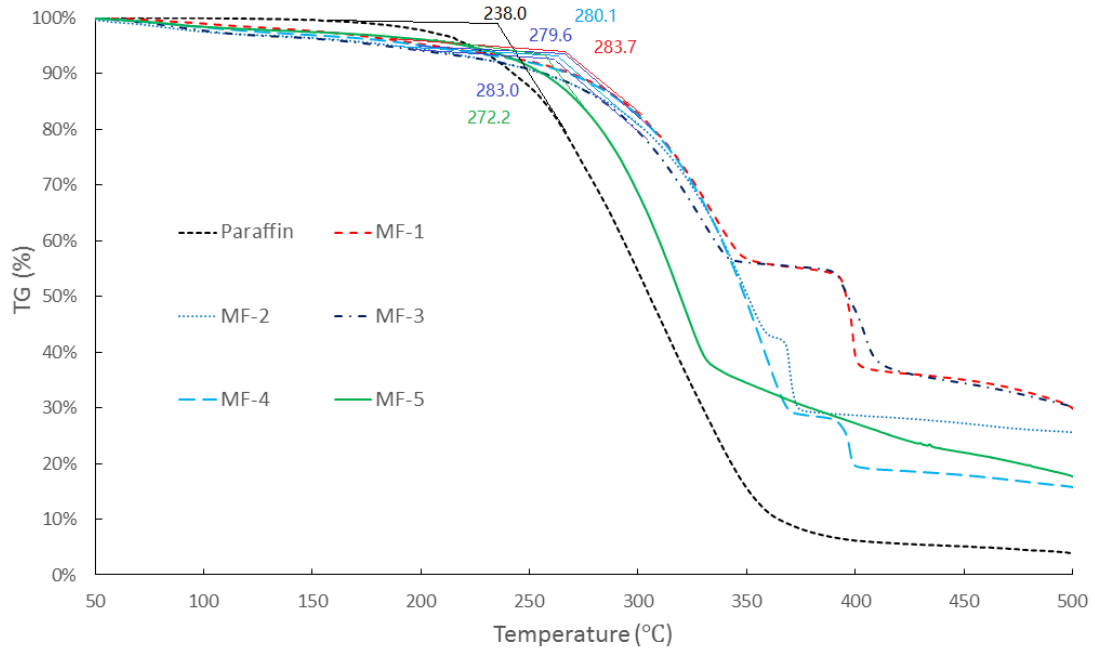


Figure 6: TG analysis of pure paraffin and MEPCM samples

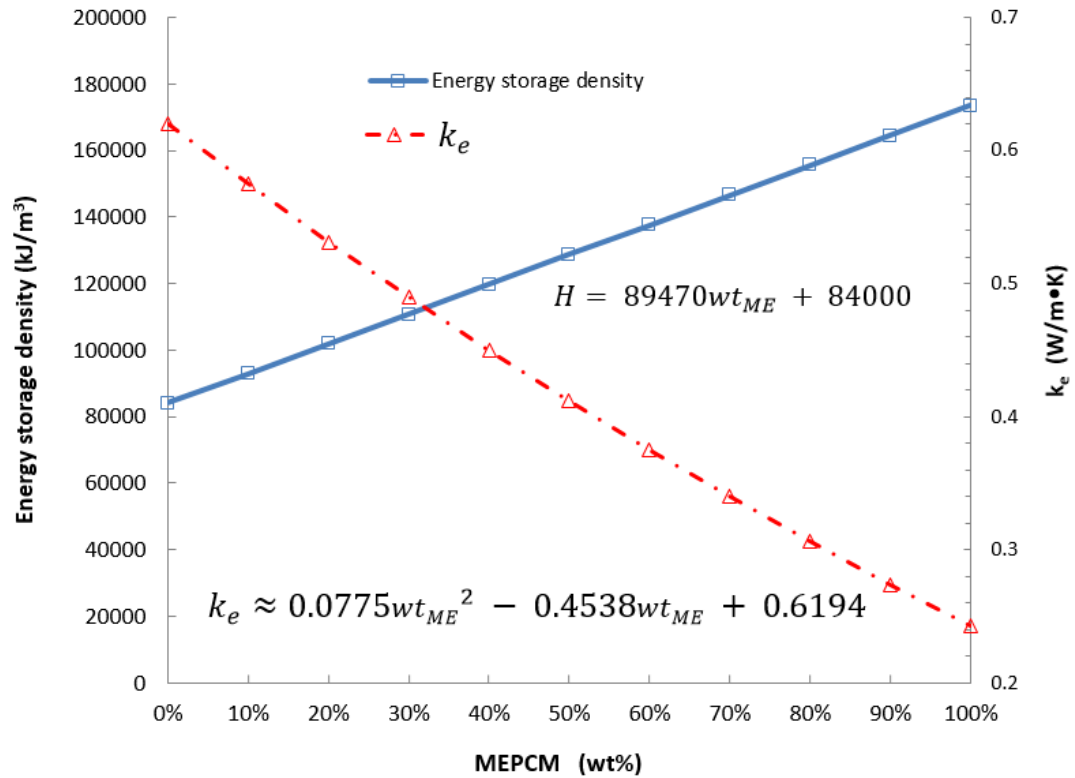


Figure 7: Thermal profile of TES unit

Table 1: Materials for MEPCM fabrication

MEPCM samples	Melamine (g)	Formaldehyde solution (g)	Emulsifier (g)	PCM (g)	Ammonium chloride (g)
MF-1	4.04	6.5	SDS (0.5)	10	0
MF-2	4.04	6.5	SDS (0.5)	10	0.125
MF-3	4.04	6.5	SDS (0.5)	10	0.25
MF-4	4.04	6.5	Brij30 & Brij58 (0.17:0.33)	10	0
MF-5	4.04	6.5	Brij30 & Brij58 (0.17:0.33)	10	0.25

Table 2: Thermal properties of paraffin and MEPCM samples

Name	Melting temperature (°C)	H (kJ/kg)	Core ratio (%)	Encapsulation efficiency (%)	Weight loss temperature (°C)
Paraffin	48.34	194	—	—	238.0
MF-1	48.25	57	29%	44.23%	283.7
MF-2	47.98	84.3	43%	65.18%	280.1
MF-3	47.66	126	65%	97.42%	279.6
MF-4	47.58	95.8	49%	74.07%	281.0
MF-5	47.39	104	54%	80.41%	272.2

Table 3: Thermophysical properties of TES components

Name	Density (kg/m <sup>3</sup> )	Cp (J/kg·°C)	Thermal conductivity (W/m·K)
Water	1000	4200	0.62
Paraffin	800	2500	0.2
MF resin	1500	1200	0.35

## Highlights

- The nucleating agent increased core material content and encapsulation efficiency
- The binary emulsifier did affect the morphology of the capsules
- The MEPCM packed bed unit did increase the energy storage density

ACCEPTED MANUSCRIPT